

Ocean-Atmosphere Mechanisms Influencing Rainfall on the Northeast of Brazil

Yves K. KOUADIO^{1,4}, Jacques Servain^{2,4*},
Luiz A.T. Machado³ and Sergio Sombra⁴

Submitted to Journal of Climatology

May 2009

¹ University of Cocody, Laboratoire de Physique de l'Atmosphère, UFR-SSMT, 22 BP 582 Abidjan 22, Côte d'Ivoire. *Visiting Scientist at CPTEC/INPE, Cachoeira Paulista, SP, Brazil.*

² Institut de Recherche pour le Développement (IRD-UR182), *Visiting Scientist at Fundação Cearense de Meteorologia e Recursos Hídricos (FUNCEME), Av. Rui Barbosa 1246, Fortaleza, CE, Brazil.*

³ Centro de Previsão de tempo e Estudos Climáticos /Instituto Nacional de Pesquisas Espaciais - CPTEC/INPE, Rodovia Pres. Dutra, km 40, Cachoeira Paulista, SP, Brazil.

⁴ Fundação Cearense de Meteorologia e Recursos Hídricos (FUNCEME), Av. Rui Barbosa 1246, Fortaleza, CE, Brazil.

* Corresponding author: Jacques Servain, Institut de Recherche pour le Développement (IRD-UR182), *Visiting Scientist at Fundação Cearense de Meteorologia e Recursos Hídricos (FUNCEME), Av. Rui Barbosa 1246, Fortaleza, CE, Brazil.*
e-mail: jacques.servain@gmail.com

Abstract

We investigate the relationship between simultaneous occurrences of intense mesoscale convective systems (MCSs), distinctive atmospheric easterly waves (AEWs) signatures and large sea surface temperature (SST) anomalies over the tropical Atlantic, and subsequent strong rainfall episodes (> 10 mm/day) over the eastern Northeast Brazil (*Nordeste*). A diagnostic analysis is firstly performed. Eleven events are selected as representative of such relationship during the *Nordeste* rainfall season (January–June) in 2004 (5 events), 2005 (4 events) and 2006 (2 events). The selected AEWs are those with a lifespan greater than or equal to 3-day, and which initiate at east of 20°W , *i.e.* far from the *Nordeste*. In a second part of the analysis, a Regional Atmospheric Modelling System (RAMS) is forced by observed SST over the tropical Atlantic for twice episodes chosen among the eleven selected events. It is found that atmospheric variables, such as equivalent potential temperature, latent heat flux, water vapour, vertical vorticity, and zonal wind, support the genesis of the strong rainfall episodes over the eastern *Nordeste* which are related to tropical Atlantic conditions which occur just a few days before. That could help in the forecasting of such dramatic episodes.

Key-Words: Nordeste, Northeast Brazil, Tropical Atlantic, Easterly Waves, Mesoscale Convective Systems, RAMS, SST

Introduction

The Northeast region of Brazil (hereafter called *Nordeste*, according to its local denomination) is located between the parallels 01° and 18°S and the meridians 35° and 47°W (Fig. 1a). The climatic mode is semi-arid for more than 80% of the area, and the region often experiences dramatic drought occurrences (Hastenrath, 1990). The *Nordeste* possesses an extensive coast along the Atlantic Ocean, and thus its rainfall regime is mainly under the influence of the tropical oceanic climate and its own variability (Markham and MacLain, 1977; Hastenrath and Heller, 1977; Moura and Shukla, 1981; Rao et al., 1996; Nobre and Shukla, 1996). The rainy season occurs generally from February to May, but however with extensions of a few weeks before or after this period according to specific sub-regions. This seasonality is mainly explained by three important atmospheric processes.

The first process is the southward seasonal migration across the equator of a zonal band of rainfall, linked to the Inter-Tropical Convergence Zone (ITCZ). The ITCZ reaches its southernmost latitude in March-April in response to the seasonal warming of the adjacent tropical Atlantic Ocean. Accordingly, the southward movement of the ITCZ, and in turn the timing and intensity of precipitation over *Nordeste*, are deeply affected by departures of sea surface temperatures (SST) from their usual seasonal changes over the tropical Atlantic. Such physical behaviour is especially important for the Northern sub-region of *Nordeste*.

The *Nordeste* rainy season is also often modulated by the northward incursion of cold fronts coming from the south tropical Atlantic. These cold fronts, linked to the strength of the episodic South Atlantic Convergence Zone (SACZ), cross the *Nordeste* in the north-westward direction from its southern coastline (8°-12°S) (Kousky and

Ferreira, 1981). These events generate atmospheric instability and contribute to increase precipitation in the full *Nordeste*, especially in its Southern sub-region.

The atmospheric easterly waves (AEWs) which cross the south-equatorial Atlantic basin from West Africa to South America (Diedhiou et al., 1998, 1999) constitute a third process which contributes to influence the seasonal rainfall mode of *Nordeste*. These waves are often associated to clusters of well defined convective systems (Yamazaki, 1975) which also propagate westwards above the equatorial basin and then contribute to locally rise the rainfall. For instance, Hall (1989) showed a relationship between the passages of AEWs and strong precipitations over Ascension Island ($7^{\circ}55$ S, $14^{\circ}19$ W) during March-to-May. More recently, Silvestre (1996) noted that such atmospheric perturbations could reach the *Nordeste*. This last phenomenon, which is especially important for the rainfall in the Eastern sub-region of *Nordeste* (Yamasaki, 1975; Yamazaki and Rao, 1977; Chan, 1990), is the focus of our present investigation. Let's note that we defined here the Eastern *Nordeste* as the region between 40° W- 35° W; 12.5° S- 2.5° S (Fig. 1a).

In a first step of the study, a diagnostic analysis is undertaken to estimate the relationship between strong precipitation episodes over the Eastern *Nordeste* and quasi simultaneous occurrences of MCSs and AEWs over the Southern Equatorial Atlantic. Eleven cases are selected and documented during the first semesters of 2004, 2005, 2006. Possible associated oceanic conditions, such as sea surface temperature (SST) patterns anomalies, are also taken into account and commented.

In a second part of the study we use the outputs of a Regional Atmospheric Modelling System (RAMS), forced by the observed SST during the same years 2004-2006, to highlight the discussion of such relationship.

Used data sets, as well as the diagnostic methodology, are presented in the next Section. The diagnostic analysis based on observations is described and discussed in the third Section. Further elements of information and discussion from the numerical experiment are presented in the fourth Section. A conclusion is finally provided.

2) Data and method

The observed daily precipitation over the *Nordeste* comes from two data sets. For the Eastern *Nordeste*, the 2004-2006 *in-situ* daily data set originates from an array of 682 meteorological stations (various data sources; see the Acknowledgments), with a higher spatial density in the coastal region, especially at east of 37°W (Fig. 1a). The Global Precipitation Climatology Project (GPCP) data set (Huffman et al., 1997) is extracted on a 1°x1° regular grid for the period 1997-2006 above the full *Nordeste*. This daily data set is deduced from a blending combination of *in-situ* observations and microwave measurements carried out by various geostationary satellites. On the continent, where the microwave emission at the surface is heterogeneous, the measurements at the frequency 85 GHz are combined with infra-red radiances to produce the estimation of daily rainfall. Though the spatial repartition of the data are quite different between these two data sources, the raw averages of monthly rainfall performed in the same area (limited here by the *in-situ* data source; Fig. 1a) show a similar evolution during the study period 2004-2006 (Fig. 1b). Many characteristics deserve to be discussed on this figure. First, though the seasonality is obvious (largest precipitations during the first semester, very few rainfall during the rest of the year), important inter-annual and intra-seasonal signals develop. Note for instance, the

exceptional high value of precipitation in January¹ 2004 (~ 12 mm/day, *i.e.* the double of the maximum generally recorded during the rainy season), or its relative low value in April 2005 (the half of March and May values for the same year).

MCSs are usually identified on the ocean by the satellite digital images in the thermal infra-red channel (Houze, 1977; Velasco and Fritsch, 1987; Mathon and al., 2002). In this study, we use the Météosat-7 images on the area 25°N-25°S, 35°W-20°E during the period January 2004 to May 2006. These data are processed and archived at *Centro de Previsão do Tempo e dos Estudos Climáticos* of *Instituto Nacional de Pesquisas Espaciais* (CPTEC/INPE) and are available each 30-minute with a space resolution of 5 km x 5 km. During its life cycle (generally from 1-to-4 days), each MCS can move, change, grow, decrease, split or merge in one or more systems. It is thus necessary, if one wants to track in space and time each event during its full lifespan, to use a method which is able to adapt to successive characteristic changes of the MCSs. ForTraCC, the model which was developed at CPTEC/INPE to extract the physical characteristics of each one of the MCSs during its life cycle, is used here to track the convective systems. This model comes from former works completed by various authors (Machado and Rossow, 1993; Machado and al., 1993, Machado and al., 1998; Mathon and Laurent, 2001; Machado and Laurent, 2004). We are using here an adaptation of the original ForTraCC for an application over the ocean. More information about the present adaptation is available in a companion paper (Kouadio et al., 2009). A few Météosat-7 images unfortunately were not available during the study period (January 2004 – June 2006). As a consequence, the output files of the ForTraCC model contain several missing data during the following periods: Jan01-Feb16 2004,

¹ January is considered as not belonging to the main rainfall season

Feb22-Feb28 2004, May05-May31 2004, Jan01-Feb15 2005, and Apr05-May18 2006. The analysis is thus only focused only on the available data sets.

The AEWs are generally depicted thanks to the relative vorticity computed from the wind field at 700 hPa (Molinari et al., 2000; Berry and Thorncroft, 2005). Here we extracted these data from the National Center for Environmental Prediction - National Center for Atmospheric Research (NCEP-NCAR) 1948-2006 reanalysis. Those daily data are reported on a $2.5^{\circ} \times 2.5^{\circ}$ grid.

A possible impact of oceanic conditions on the *Nordeste* rainfall is study by using daily SST fields from 2004 to 2006. Those data provided on a $0.25^{\circ} \times 0.25^{\circ}$ grid, is given by the Institut Français de Recherche pour l'Exploitation de la Mer (Ifremer) on its website (www.ifremer.fr/).

In order to highlight the diagnostic approach, a set of atmospheric circulation simulations was carried out by using the Regional Atmospheric Modelling System (RAMS) previously developed by several worldwide groups, including at Colorado State University and Atmospheric Meteorological and Environmental Technology (ATMET). That regional model can be used for various objectives, from the study of local physical processes to the forecasting of regional seasonal climate. The RAMS was adapted at *Fundação Cearense de Meteorologia e Recursos Hídricos* (FUNCEME) to focus on the atmospheric circulation over the *Nordeste*, and it is now regularly used (from January of each year) to forecast the subsequent rainy season over the region. The daily SST fields grid provided on a $0^{\circ}25 \times 0^{\circ}25$ by Ifremer served here to force the RAMS during the period 2004-2006. The numerical simulation produced several atmospheric parameters in a grid of 25 x 25 km, with a time step of one hour according to 14 pressure levels fom 1000 hPa to 50 hPa. The RAMS was carried out by using the

diagrams of convection parameterization proposed by Kuo (Kuo, 1974; Molinari, 1985) in order to better reproduce the precipitation fields on the continent. In our specific simulated experiment we are especially interested by: (i) how the atmospheric conditions evolve/move according to the SST variability; and (ii) how this ocean-atmospheric coupling can influence strong rainfall episodes over Eastern *Nordeste*. Two specific examples during the study periods are presented in Section 4.

3) Diagnostic analysis

Figure 2 illustrates two examples of the good relationship between the *Nordeste* precipitation and AEW and MCS indices over the tropical Atlantic basin. The rainfall (mm/day) is monthly averaged from the GPCP climatic data over the domain 2.5°S-12.5°S, 40°W-35°W, which largely includes the Eastern *Nordeste*. The AEW monthly index is computed by averaging the positive vorticity at 700 hPa over the region 2.5°S-12.5°S, 40°W-20°E. More precisely, Figure 2a shows that the AEW monthly intensity over the ocean, averaged over the 1948-2006 period, is clearly higher (x 1.5 times) during the first semester (especially in March-April-May), *i.e.* during the regular rainfall season over the *Nordeste*, that during the rest of the year. Such evidence of higher values in the positive vorticity during the first months of the year remains the same when individual years 2004, 2005 and 2006 (Fig. 2b) are plotted.

A MCS monthly index is also given from 2004 to the first semester of 2006 (see the dashed dotted curve in Fig. 2b). This index represents the total number of MCSs (lifespan > 2 hours) selected by ForTraCC from the available Meteosat imagery² which move in the westward direction inside the region 35°W-20°W, 2.5°S-12.5°S. The

² Index value not plotted when there is a lack of data higher than 15 days during a given month.

seasonal evolution of the MCS index is similar to that ones of *Nordeste* precipitation (continuous line on Fig. 2b) and AEW index (dotted line on Fig. 2b): a higher (lower) number of MCSs is generally associated with abundant (sparse) precipitation over the *Nordeste*, and stronger (weaker) positive vorticity. That validates the good relationship between westwards MCSs and AEW occurrences over the tropical Atlantic and the seasonal rainfall over Eastern *Nordeste*.

Examples of MCS westward trajectories in the area 12.5°S - 5°N , 35°W - 20°E are shown in the three panels of Figure 3 for the periods January-to-May in 2004, 2005 and 2006 (panels a, b, and c, respectively). For clearness of the figure, only the MCSs whose life cycles were higher than 10-hour and whose which dissipated between 12.5°S and 2.5°S of latitude were selected. Neither the curves of trajectories, nor the spreading surfaces of the MCSs are represented, but rather the initiation and dissipation coordinates which are linked by a straight line. For reference, we defined the initiation (dissipation) coordinates as being the position of the MCS in the first (last) available image where the brightness temperature is lesser (greater) than the used threshold (*e.g.* Kouadio et al., 2009). This figure shows that the MCSs are essentially spreading according to three regions. Two first regions have a larger density and a larger meridional extension (5°N - 20°S): one on the West African continent, with a westward extension up to 5°E , and another one at west of 20°W which reaches the South American continent. The third region, with a weaker density, is trapped along a zonal band between Equator and 5°S , from 5°E to 20°W . Such MCS successive occurrences during the period JFMAM could show a regeneration of the systems by multiple phenomena of merge or split. It is interesting to note (not shown) that practically none MCS event moving westward occurred in that equatorial region during the period from

June to January. Another double remark: (i) all MCSs initiated in Africa dissipated towards 5°E and never reach the *Nordeste*; (ii) all the convective systems whose dissipation coordinates reached (or nearly reached) the South American continent, initiated on average at west of 20°W . In this region close to *Nordeste*, the MCSs which initiated in the north of 5°S often combined with those which initiated in the south of this latitude. Between 20°W and 5°E , the lack of MCS in the Southern basin at south of 5°S indicates a zone of subsidence.

Figure 4 represents the positive daily vorticity at 700 hPa averaged between 2.5°S - 12.5°S of latitude along 40°W - 20°E of longitude for the three periods JFMAMJ of each year 2004, 2005, and 2006 (panels a, b and c, respectively). Several AEW trains crossed the Atlantic basin, most of them from Africa to South America. Occurrences of strong positive anomaly of daily (GPCP) precipitation (> 10 mm/day) over the Eastern *Nordeste* are indicated on the figure by dots along the meridian 36°W , *i.e.* about the mean latitude of this sub-region (Fig. 1). These rainfall anomalies are the differences between the daily values of the rainfall averaged inside the domain 2.5°S - 12.5°S , 40°W - 35°W and the climatology precipitation associated to the same calendar days averaged over the same region during the period 1997-2006 (see also Fig. 5). Although several strong rainfall anomalies (> 10 mm) experienced during the study period, only a part of them seemed directly related to AEWs. That is exactly these last episodes we are focusing on. Such twice diagnostic schematization focused here allowed to identifying a few AEW occurrences which seemed to be in relationship with short episodes of strong precipitation over the *Nordeste*. The research of these events was completed by the following: we only selected the AEWs (i) which reached (at least) the coast of *Nordeste* (*i.e.* 36°W) at the date of the noted strong rainfall episodes, (ii) which were initiated (at

least) at east of 20°W , and (iii) of which the lifespan was higher or equal to 3-day. This simple technique highlighted eleven cases, of which five in 2004, four in 2005 and two in 2006. These waves, schematically indicated on the figure by dashed lines from the initiation spots to the rainfall event spots, have a phase speed ranging between 5-to-11.9 m/s and a period ranging between 3-to-8 days (see Table 1). Let's take in mind that the initiation date of the AEW event is considered as being the date at which the wave signature is observed as shown in the Table 1. All the waves initiated in the open ocean, at west of 5°E , *i.e.* above supposed subsidence areas. That indicates the existence of a certain convective activity, even if that is not easy to locate it thanks to satellite images.

Note that Figure 4 also shows that several positive strong positive rainfall anomalies over the *Nordeste* which do not seem associating with episodes of AEW propagations (Figs. 4 & 5). That certainly may be explained by the influence of other ocean-atmosphere physical processes, such as those already discussed in the Introduction section, as for instance the migration of the ITCZ, or incursions of cold fronts coming from South Atlantic (*e.g.* Kousky and Ferreira, 1981).

4) Numerical analysis

A RAMS simulation, forced by the previously SST [qu'est-ce que ça veut dire "previously SST" ??? être plus précis ...], is carried out during the 28 May to 01 Jun 2004 event and during the 10-15 Feb 2005 event (cf. Table 1) to understand the mechanisms that could help by triggering and sustaining the selected events. These events are noted N°1 and N°2 on Figure 4 respectively. [il serait quand même utile de dire pourquoi on focus ici sur ces deux évènements, et pas sur les autres Qu'ont-ils

de si particuliers que ça ??? Ou bien, au contraire, peut-on considérer qu'ils "synthétisent" l'ensemble des 11 sélections ?? Ou encore qu'ils représentent deux familles de cas ?? Par ailleurs il ne faut pas commencer ce chapitre en disant « A RAMS simulation .../... is carried out during » dire que le RAMS a été utilisé pour l'ensemble des 11 évènements ... et que nous ne discutons ici que les deux évènements 1 et 2 parce que, et parce que, etc ... voir plus haut ...]. **The convective scheme of Kuo (1974) is used in the simulation** [phrase à mettre dans la description du modèle, pas ici].

The two selected events occurred practically at the beginning (N°2) and at the end (N°1) of the rainy period. [pourquoi, alors, n'avoir pas choisi un troisième cas, au milieu de la saison des pluies ??]. The EAWs associated to these two events initiated over the centre of the ocean basin ($\sim 5^\circ\text{W}$) or close to the African coast, for N°2 and N°1 cases respectively, *i.e.* far from the coastal zone of frequently convection of the *Nordeste*. The precipitation anomaly patterns (not shown [pourquoi ??? ça serait pourtant hyper-intéressant de montrer ça !!!]) exhibit positive structures on the *Nordeste* domain, with high values at the most eastern side (~ 30 mm/day for the case N°1) and in the southern part (~ 30 mm/day for the case N°2). When averaging on the whole *Nordeste* domain, the precipitation anomalies for the both cases (16.3 mm/day for the case N°1 and 15 mm/day for the case N°2) are approximately around the average of the eleven selected events (~ 15.9 mm/day). The AEW durations of the both events (4 days for the case N°1 and 5 day for the case N°2) also resemble the average of the eleven events (~ 4.8 days).

The both events present different evolutions of the daily SST anomaly patterns (Fig. 6) [en noir & blanc c'est très difficile de distinguer les valeurs positives et négatives ... pourquoi ne pas mettre de la couleur ?? Par ailleurs, et ainsi que je te l'ai déjà dit ... je ne suis pas sur que ça soit la solution la plus judicieuse de montrer les

anomalies de SST exactement au même moment -même si tu commence un jour avant- que les évènements atmosphériques ... à mon avis il faudrait voir comment sont les anomalies de SST plusieurs jours AVANT Comme je te l'ai déjà dit aussi ... T'as regardé ça ?? Si on pouvait montrer qu'il y a eu un refroidissement -par évaporation- qui a suivi, quelques jours plus tard, un réchauffement anormal ... ça aurait plus de gueule, non ? En ce cas il ne faudrait pas montrer une image par jour, mais une tous les 3 ou 4 ou ? jours ...] The daily SST anomalies are calculated as the differences between the daily values and the climatology SST associated to the same calendar days averaged during the period 2004-2006. The SST anomalies patterns are plotted one day before the date of the initiation of the event up to the rainy day. This is done to show the oceanic warming, and then the evaporation that could exist before the AEW initiation [OK, mais à mon avis, ça doit se faire sur une période plus longue, non ?]. The case N°1 is related to a cooling [tu vois ? où est le réchauffement "initial" ??] that intensifies until June 01. This means that the ocean continues to loose energy since the event initiation. The warming structures observed southward of 8°S, during May 27 and May 28, close to the African coast up to 20°W of longitude disappear progressively. In the meantime, an ocean warming ($< 0.2^{\circ}\text{C}$) is located along the *Nordeste* coast, between 33°W and 35°W on June 01[un peu tiré par les cheveux cette argumentation même en se référant aux figures en couleur (plus lisibles) du ppt !!!]. In the case N°2, a general warming occurs in the whole southern basin with high values ($> 0.6^{\circ}\text{C}$) between 10°W and the African coast during Feb 09 to Feb 11. Although cooling structures are observed from Feb 13 to Feb 15 in certain parts of the ocean, the warming remains persistent in the southern Atlantic Ocean. [Ouais J'suis pas trop convaincu]

Figure 7 shows the vertical profiles from 1000 to 200 hPa of the equivalent potential temperature (θ_e) for the both events averaged inside the oceanic domain 35°W-10°E, 2.5°S-12.5°S. Figures 7a and 7b are related to the case N°1 and to the case N°2 respectively. θ_{e1} represents the equivalent potential temperature at the two initiation dates of the AEW whereas θ_{e2} is the date of the two strong rainfall events over the eastern *Nordeste* (see Table 1). The two differences between θ_{e2} and θ_{e1} are also plotted (Fig. 7c). There show how the daily variation of SST (see Fig. 6) could impact convection through the vertical structure of the atmosphere [là tu t'avances sérieusement !!! ... ton interprétation ... à partir uniquement de la SST ... est assez osée, non ??]. It is apparent that in the both cases, change is observed in the stability of the atmosphere. Positive difference between θ_{e2} and θ_{e1} is noted in the lower layers with high values approximately at 700 hPa. There show an input of moisture from the lower layers which helps to increase the humidity of the atmosphere and influence the precipitation over the *Nordeste*. [ouais !!!! bof !!! pas trop convaincu ...] [et la différence, elle aussi positive, dans les hautes couches ?? vers 400hPa ... t'en parles pas ??]

Figure 8 shows the daily evolution of latent heat flux (LH) averaged over the latitudinal band 2.5°S-12.5°S for the both cases. This evolution is obtained from the difference between every day and the initiation day of a studied event. The reason is to overcome the lack of the output climatologically data of the RAMS necessary to calculate a real anomaly. This calculation is used to show the daily behaviour of the atmospheric variable when taking the initiation day of the event as the reference. An excess of LH is noted practically in the ocean two days after the initiation of each event. [pas évident ... !!] For the case N°1, it occurred during May 29 to May 30 while it is

observed from Feb 11 to Feb 12 for the case N°2 [j'aimerais bien voir les résultats si tu prends une référence AVANT les 28 mai 2004 et/ou 10 février 2005]. A decrease of LH that intensifies and extents in the ocean the last days of the events may be related to the cooling of the ocean (see Fig. 6). These remarks (for both cases) indicate that the heat stored in the ocean surface contributes, by evaporation, to moisten the atmosphere and to create an environment conducive to the formation of convective systems. [ouais ... pt'êt ??] This assertion is consistent with Rotunno and Emanuel (1987) and Tao et al., (1991) who noted the importance of the heat flux which carries the humidity that could help for the development of convection and precipitation. In addition, the longitudinal intensification and extension of the heat transported into the atmosphere by the ocean could help to increase atmospheric instability. This action, if any, could be associated with an intensification of trade winds toward the *Nordeste*, a cooling of ocean surface and thus induce an increase in precipitation. [pt'êt ??...]

Figure 9 represents the Hovmöller time-altitude diagram of the vertical vorticity averaged over the oceanic domain 35°W-10°E, 12.5°S-2.5°S for the two cases. It illustrates the vertical motion of the moisture in the atmosphere. A negative value indicates an upward motion that carries moisture to the troposphere, while a positive value indicates the opposite. In the both cases, a vertical ascent is **observed** [tu ne peux pas parler d'observation dans le cas d'une simulation !!] ~~during the event periods.~~ It is ~~localized~~ **simulated** in the lower layers. It is localized from the ocean surface to about 850 hPa during cases N°1 and N°2. That means that during these two events, evaporation coming from the ocean is transported upward to the atmosphere. The moistened air near the surface converges into the atmospheric circulation and help in

releasing the latent heat ascent. [et pour les niveaux au-dessus ... ex. valeurs négatives ... on ne donne aucune discussion ??]

Water vapour simulated by the model for the both cases is illustrated by the daily evolution of the difference between every day and the initiation day of a studied event (Fig. 10). The water vapour is averaged over the latitudinal band 2.5°S-12.5°S. These panels show that the water vapour is present throughout the atmospheric column with a progressive rise into the 800-600 hPa band centred at 700 hPa. The presence of water vapour at the surface is consistent with the ascending motion shown in Figure 9. At 700 hPa, the increase of water vapour could suggest its reinforcement during the westward spread of the AEW related to the strong rainfall episode. When looking on the both events, a progressive disappearance of the positive water vapour difference **observed [!!!]** near the *Nordeste* coast in the lower levels, between 1000 to 800 hPa associated with an increase of water vapour during the rainy day over the *Nordeste*. [phrase complètement incompréhensible]

Figure 11 shows the Hovmöller altitude-longitude diagram of the zonal wind simulated by the model for the both cases. It is averaged over the latitudinal band 12.5°S-2.5°S along 40°W-15°E of longitude. Pressure levels from 1000 to 200 hPa represent altitudes. These panels illustrate the daily evolution of the zonal wind forced by the daily variation of the SST [?? La SST qui force l'atmosphère jusqu'à 200 hPa ?? Là il y a un gros problème de discussion/interprétation !!]. The simulation allows studying the moisture advection from the ocean to the continent. The same calculation as for Figure 10 is performed here. The negative (positive) value indicates a westward (eastward) advection. The figure shows that the atmospheric circulation helps to transport the moisture flow from the ocean to the *Nordeste*, with a marked difference

between the two events. In the case N°1, the horizontal transport [ça manque de précision de dire ça car les figures représentent des différences de vitesse !!!] is located between 1000 to 500 hPa. In the case N°2, the horizontal transport [??? même remarque ...] is localized between the 1000 and 300 hPa levels. The negative differences of the zonal wind located at these levels, reach their maximum, near the *Nordeste*, around Feb 13 2005 between 35°W to 30°W of longitudes and fade gradually until the rainy day. However, the negative differences of the zonal wind cover the entire *Nordeste* in the 2004's case (specifically on May 30 to 31) while they remain confined around 37°W in the 2005's case. This could explain the higher positive anomaly of GPCP precipitation on June 01 2004 (~ 16 mm) than on Feb 15 2005 (15 mm) [SEULEMENT 1mm de différence !!!! absurde de dire ça !!!]. Note that during the both events, the advection of moisture towards the *Nordeste* in the lower layers (from 1000 hPa to 700 hPa) does not exist virtually on the rainy day. It is possible that the moisture that could impact on the MCSs formation, and therefore on the rain, is advected one day before. [toute cette discussion, sur le vent zonal, me semble vraiment sous-argumentée]

Finally, the last step of the simulation shows the evolution of the daily water vapour mixing ratio (WVIR) associated to the rainfall in the *Nordeste* for the both cases. We note an increase of WVIR on the *Nordeste* from May 30 2004 for event N°1, and from Feb 13 2005 for event N°2 (Fig. 12). The lower value observed on case N°1 compared to that case N°2 could also explain the differences between the horizontal transport during these days as previously noted: the horizontal transport of the water vapour covers the *Nordeste* in the case N°1 while it remains towards 37°W in the case N°2. In addition, the progressive increase of the WVIR on the continent is consistent with decrease of the latent heat, the gradual decrease of the water vapour over the ocean

and the strong advection the previous days before the rainy day in the *Nordeste*. [cette figure me semble nettement plus convaincante que les deux précédentes ...]

5) Summary and conclusion [anglais à revoir ...]

Previous studies enumerate and discuss the physical processes that could affect the precipitation in the *Nordeste*, as for instance the seasonal migration of the ITCZ, the northward incursion of cold fronts coming from the South Atlantic, and atmospheric easterly waves (AEW) propagating above the tropical Atlantic basin. Although these studies are numerous, a few of them focus on the influence of the southern hemisphere AEWs on the *Nordeste* precipitation. Here, we attempted to ascertain [??] the action of these last phenomena and how they are sustained when crossing westward the south Atlantic basin. This study, if any [??], could help in the prediction of the *Nordeste* precipitation.

In order to approach this problem, we analyzed the relationship between precipitation in the eastern *Nordeste* region of Brazil (40°W-35°W; 2.5°S-12.5°S), the MCSs and the AEWs that cross the south tropical Atlantic and reach the *Nordeste* and the SST conditions over the southern equatorial basin. Our goal is to see how the daily frequency of SST variability induces strong rainfall episodes through specific weather conditions. To understand these mechanisms, a simulated numerical experience is performed using the Regional Atmospheric Model System (RAMS). Daily observed SST is used to force the atmospheric model. This study examines the period from January to June during 2004, 2005 and 2006, the first semester of the year being considered as including the seasonal rainfall over the *Nordeste*.

All the MCSs initiated in Africa which move westward are not more directly observed towards 5°E. As a result, the precipitation in the eastern of *Nordeste* seems only directly influenced by the MCSs initiated inside the region 35°W-20°W; 2.5°S-12.5°S, an oceanic zone with frequent convection occurrences. A coherent similar evolution was observed between the MCSs which move westward inside the region 35°W-20°W; 2.5°S-12.5°S up to the *Nordeste*, the horizontal vorticity over the domain 40°W-20°E; 2.5°S-12.5°S and the precipitation in the eastern *Nordeste*.

Eleven events of strong rainfall episodes over eastern *Nordeste* (daily anomaly > 10 mm) are selected during the first semesters of 2004, 2005 and 2006 using a simple diagnostic technique. The selected AEW signatures associated to these events are those that reach at least the mean eastern longitude of *Nordeste* (*i.e.* 36°W) during the selected rainy days, which are initiated at east of 20°W, and of which lifespan is at least greater than or equal to 3-day. The wave signatures are calculated in the latitudinal band 12.5°S-2.5°S and are indicated by the longitudinal spread of the vorticity at 700 hPa. It is shown that among the strong rainfall anomalies episodes which occurred in first semesters 2004, 2005 and 2006, and several of them are related to AEWs. We hypothesized that the others strong rainfall episodes may certainly be influenced by others physical processes as for instance the migration of ITCZ or introducing of cold fronts.

The RAMS is especially used during two different events located at the beginning (10-15 February, 2005) and at the end (May 28-June 01, 2004) of the main seasonally rainy period. These events present (*i*) waves initiated over the middle of the ocean and at the African coast respectively, (*ii*) different evolutions of the daily SST anomaly patterns and (*iii*) exhibit positive structures [de quoi ???] on the *Nordeste*

domain. Change in atmospheric conditions [jusqu'à 200 hPa ???] was forced by the daily variation of SST.

During the westward spread of the AEWs, a daily decreasing in LH is observed on the open ocean up to the *Nordeste* coast. It is hypothesized [il faut prendre ses responsabilités, mon gars !!!] that the latent heat could help in moistening the atmosphere, to create an environment conducive to the formation of convective systems and then to increase atmospheric instability. The loss of LH is found to be consistent with the progressive cooling of the ocean. As a consequence, SST plays an important role in the increasing of atmospheric convection and formation of the MCSs. Indeed, SST variability affects directly the air temperature and moisture properties in the boundary atmospheric layer through the turbulent fluxes above the sea surface (Graham and Barnett, 1987; Zhang, 1993; Arking and Ziskin, 1994).

It was noted that the evaporation coming from the ocean is transported upward to the upper atmosphere. It implies that the air near the surface converges into the atmospheric circulation through the vertical ascent and helps in the reinforcement of the water vapour. Such upward motion in the convective activity helps by favouring the instability of the flow (Scharney and Stern, 1962). The sustaining of the westward propagation of this generated dynamical instability could be [même remarque que la précédente ...] influenced by the convection over the ocean. Finally, the vapour in the atmosphere is horizontally transported from the ocean up to the *Nordeste* by the wind and influences the precipitation. Such a mechanism of the moisture transport from the ocean to the continent, coupled with strong rainfall episode in the *Nordeste* is consistent with Brubaker et al., (1993). [ouais Ce "summary and conclusion" pourrait être amélioré fortement ... d'abord en supprimant toute la partie « summary » (une bonne

moitié) et en se concentrant uniquement sur la partie « conclusion » Et aussi en améliorant fortement l'anglais ...] [Terminer sur quelques phrases pour essayer de justifier la dernière phrase de ... l'abstract !!]

Acknowledgments: This work is part of the CNPq-IRD Project “Climate of the Tropical Atlantic and Impacts on the Northeast” (CATIN), No. CNPq Process 492690/2004-9. Y. K. K. stayed in 2007 at the *Fundação Cearense de Meteorologia e Recursos Hídricos (FUNCEME)* and was supported by the French Institut de Recherche pour le Développement (IRD) grant (2006–2007). The *in-situ* rainfall data of the Nordeste were obtained thanks to various researchers (.....). [à ne pas oublier]

References

- Arking, A and D. Ziskin, 1994: Relationship between clouds and sea surface temperature in the western tropical Pacific. *J. Climate*, **7**, 988–1000.
- Brubaker, K. L., D. Entekhabi, and P. S. Eagleson, 1993: Estimation of continental precipitation recycling. *J. Climate*, **6**, 1077–1089.
- Chan S. C., 1990: Análise de distúrbios ondulatórios de leste sobre o Oceano Atlântico equatorial Sul; São José dos Campos, (INPE - 5222-tdl/437). In portugues.
- Diedhiou, A., S. Janicot, A. Vitard and P. Felice and H. Laurent, 1999: Easterly wave regimes and associated convection over West Africa and tropical Atlantic: Results from the NCEP/NCAR and ECMWF reanalyses, *Clim. Dyn.*, **15**, 795–882.
- Diedhiou, A., S. Janicot, A. Vitard and P. Felice, 1998: Evidence of two regimes of easterly waves over West Africa and the tropical Atlantic, *Geophys. Res. Lett.*, **25**, 2805–2808.
- Graham, N. E., and T. P. Barnett, 1987: Sea surface temperature, surface wind divergence, and convection over the tropical oceans. *Science*, **238**, 657–659.
- Hall, B.A., 1989: Westward-moving disturbances in the South Atlantic coinciding with heavy rainfall events at Ascension Island. *Meteorol. Mag.*, **118**, 175-181.
- Hastenrath, S, 1990: Prediction of Northeast Brazil rainfall anomalies. *J. Climate*, **3**, 893-904.
- , and L. Greischar, 1993: Further work on the prediction of Northeast Brazil rainfall anomalies. *J. Climate*, **6**, 743-758.
- Houze, R. A. Jr, 1977: Structure and dynamics of a tropical squall-line system. *Mon. Wea. Rev.*, **105**, 1540–1567.

- Kouadio K. Y., L.A.T. Machado and Jacques Servain, 2009: Tropical Atlantic Hurricanes, Easterly Waves, and West African Mesoscale Convective Systems. *Submitted to Int. J. Climatology*.
- Kousky, V. E. and N. J. Ferreira, 1981: Interdiurnal surface pressure variations in Brazil: their spatial distribution, origins and effects, *Mon. Wea. Rev.*, **109**, 1999–2008.
- Kuo, H.L., 1974: Further studies of the parameterization of the influence of cumulus convection on large-scale flow. *J. Atmos. Sci.*, **31**, 1232-1240.
- Machado, L. A. T., J-P. Duvel, and M. Desbois, 1993: Diurnal variations and modulation by easterly waves of the size distribution of convective cloud clusters over West Africa and Atlantic Ocean. *Mon. Wea. Rev.*, **121**, 37–49.
- , R. L. Guedes, and A. W. Walker, 1998: Life cycle variations of mesoscale convective systems over the Americas. *Mon. Wea. Rev.*, **126**, 1630–1654.
- , and W. B. Rossow, 1993: Structural characteristics and radiative properties of tropical cloud clusters. *Mon. Wea. Rev.*, **121**, 3234–3260.
- , and H. Laurent, 2004: The convective system area expansion over Amazonia and its relationships with convective system life duration and high-level wind divergence. *Mon. Wea. Rev.*, **132**, 714–725.
- Mathon, V., and H. Laurent, 2001: Life cycle of the Sahelian mesoscale convective cloud systems. *Quart. J. Roy. Meteor. Soc.*, **127**, 377–406.
- , H. Laurent, and T. Lebel, 2002: Mesoscale convective system and rainfall in the Sahel. *J. Climate*, **141**, 1081–1092.
- Markham, C.G. and D.R. MCLAIN, 1977: Sea surface temperature related to rain in Ceará, northeastern Brazil. *Nature*, **265**, 320-323.
- Molinari, J., 1985: A General form of Kuo's Cumulus Parameterization. *Mon. Wea. Rev.*, **113**, 1411-1416.
- Moura, A. D. and J. Shukla, 1981: On the dynamics of droughts in northeast Brazil: Observation, theory, and numerical experiments with a general circulation model, *J. Atmos. Sci.*, **38**, 2653–2675.
- Nobre, P. and J. SHUKLA, 1996: Variations of sea surface temperature, wind stress, and rainfall over the tropical Atlantic and South America. *J. Climate*, **9**, 2464-2479.

- Rao, V. B., I. Cavalcanti, and K. Hada, 1996: Annual variations of rainfall over Brazil and water vapor characteristics of South America. *J. Geophys. Res.*, **101**, 36 350–36 551.
- Routunno, R. and K.A. Emanuel, 1987: An air-sea interaction theory for tropical cyclones. *J. Atmos. Sci.*, **44**, 542–561.
- Silvestre E., 1996: Distúrbios nos Ventos de Leste no Atlântico Tropical, São José dos Campos, INPE. In portuguese.
- Tao, W.-K., J. Simpson and S.-T. Soong, 1991: Numerical simulation of a subtropical squall line over the Taiwan Strait. *Mon. Wea. Rev.*, **119**, 2699–2723.
- Velasco, I., and J. M. Fritsch, 1987: Mesoscale convective complexes in the Americas. *J. Geophys. Res.*, **92**, 9591–9613.
- Waliser, D. E., 1996: Formation and limiting mechanisms for very high sea surface temperature: Linking the dynamics and the thermodynamics. *J. Climate*, **9**, 161–188.
- Wallace, J.M. and C.P. Chang, 1969: Spectrum analysis of large scale wave disturbances on the tropical lower troposphere. *J. Atmos. Sci.*, **26**, 1010-1025.
- Yamazaki, Y. and V.B. Rao, 1977: Tropical cloudiness over South Atlantic Ocean. *J. Meteor. Soc. Japan*, **55**, 204-207.
- Yamazaki, Y., 1975: Estudos teóricos e snóticos dos distúrbios tropicais. São Jose dos Campos, INPE, INPE-624-LAFE. In portuguese.
- Zhang, C., 1993: Large-scale variability of atmospheric deep convection in relation to sea surface temperature in the Tropics. *J. Climate*, **6**, 1898–1913.

Figure Captions [j'ai fait des corrections/commentaires directement sur les légendes des figures, pas sur cette liste]

Figure 1: (a) Spatial distribution of 682 stations of the Nordeste. The dashed rectangle represents the eastern part of the Nordeste ranged between 40°W - 35°W of longitude and 12.5°S - 2.5°S of latitude. (b) GPCP and *in-situ* monthly rainfall 2004-2006 averaged over the Nordeste.

Figure 2: (a) Monthly climatology of GPCP rainfall (dotted line) during 1997-2006 calculated over the Nordeste and the 700 hPa positive vorticity (solid line) inside the area 40°W - 20°E , 12.5°S - 2.5°S for the period 1948-2006. (b) Monthly number of MCSs (lifespan > 2 hours), which move westward (dashed) from 20°W up to the Nordeste and have a dissipation coordinate ranged between 12.5°S and 2.5°S during 2004-2006. Monthly rainfall of GPCP (solid line) on the Nordeste monthly vorticity (dotted) on the area 40°W - 20°E , 12.5°S - 2.5°S are also plotted.

Figure 3: MCSS (> 10 hours) trajectories that move westward in the area 35°W - 20°E , 12.5°S - 5°N during January-May in (a) 2004, (b) 2005 and (c) 2006.

Figure 4 : The 700 hPa relative vorticity ($\times 10^{-5} \text{ S}^{-1}$) in January-June of (a) 2004, (b) 2005 and (b) 2006 along 40°W - 20°E averaged between 12.5°S and 2.5°S . Positive anomalies great to 10 mm/day of the GPCP (dotted) are represented on the mean eastern longitude of the Nordeste. Initiation coordinates of selected events are mark as square. The initiation of the event and the rainy day are connected by a dashed line. The vertical line represents approximately the limit ($\sim 10^{\circ}\text{E}$) of the African continent.

Figure 5: Chronological series of the daily GPCP anomalies calculated over the eastern Nordeste region (40°W-35°W; 12.5°S-2.5°S) in 2004 (top), 2005 (middle) and 2006 (bottom). The year is written at the top right side of each figure. The horizontal dashed line represents the positive rainfall anomaly great to 10 mm/day.

Figure 6: Daily evolution of the SST anomalies for the both events: (left) May 27-June 01 2004 and (right) Feb 09-Feb 15 2005 event.

Figure 7: Vertical profiles of the equivalent potential temperature averaged over the oceanic domain 35°W-10°E; 12.5°S-2.5°S for two days during (a) the May 28 -Jun 01 2004 event and (b) the Feb 10-Feb 15 2005 event. Equivalent potential temperature curve for the initiation date of each event is continuous whereas it is dotted at the end. (c) Difference between the equivalent potential temperature at the end and at the initiation dates of each event: May 28 -Jun 01 2004 (solid) and Feb 10-Feb 15 2005 (dotted).

Figure 8: Daily evolution of the latent heat differences calculated over the 12.5°S-2.5°S latitudinal band along 40°W-15°E of longitude for the both events: (left) May 28 -Jun 01 2004 and (right) Feb 10-Feb 15 2005. Positive values are shaded. The vertical dashed line represents the mean longitude (~ 36°W) of the eastern Nordeste.

Figure 9: Hovmöller time-altitude diagram of the daily evolution of relative vertical vorticity ($\times 10^{-6}$ rad s⁻¹) calculated on the oceanic domain 35°W-10°E ; 12.5°S-2.5°S for

the both events: (a) May 28 -June 01 2004 and (b) Feb 10-Feb 15 2005. Negative values are shaded.

Figure 10: Hovmöller altitude-longitude Diagram of the daily evolution of water vapour difference calculated on the 12.5°S-2.5°S latitudinal band along 40°W-15°E of longitude for the both events: (left) May 28- June 01 2004 and (right) Feb 10-Feb 15 2005. Positive values are shaded.

Figure 11: Hovmöller altitude-longitude Diagram of the daily evolution of zonal wind differences calculated on the 12.5°S-2.5°S latitudinal band along 40°W-15°E of longitude for the both events: (left) May 28- June 01 2004 and (right) Feb 10-Feb 15 2005. Negative values are shaded.

Figure 12: Daily evolution of the integrated water vapour mixing ratio (WVIR) calculated over the Nordeste (40°W-35°W ; 12.5°S-2.5°S) for the both events: May 28 - June 01 2004 (solid curve) and Feb 10-Feb 15 2005 (dashed curve). The daily scale for the period Feb 10-Feb 15 2005 (horizontal dashed line) is plotted at the bottom of the panel.

Table 1: Summary information for the 11 selected events in 2004, 2005 and 2006 when the strong anomaly of rain (> 10 mm) in the Nordeste is associated with AEWs. The mean virtual velocity (m s^{-1}), the initiation and rainy date of each event are also given.

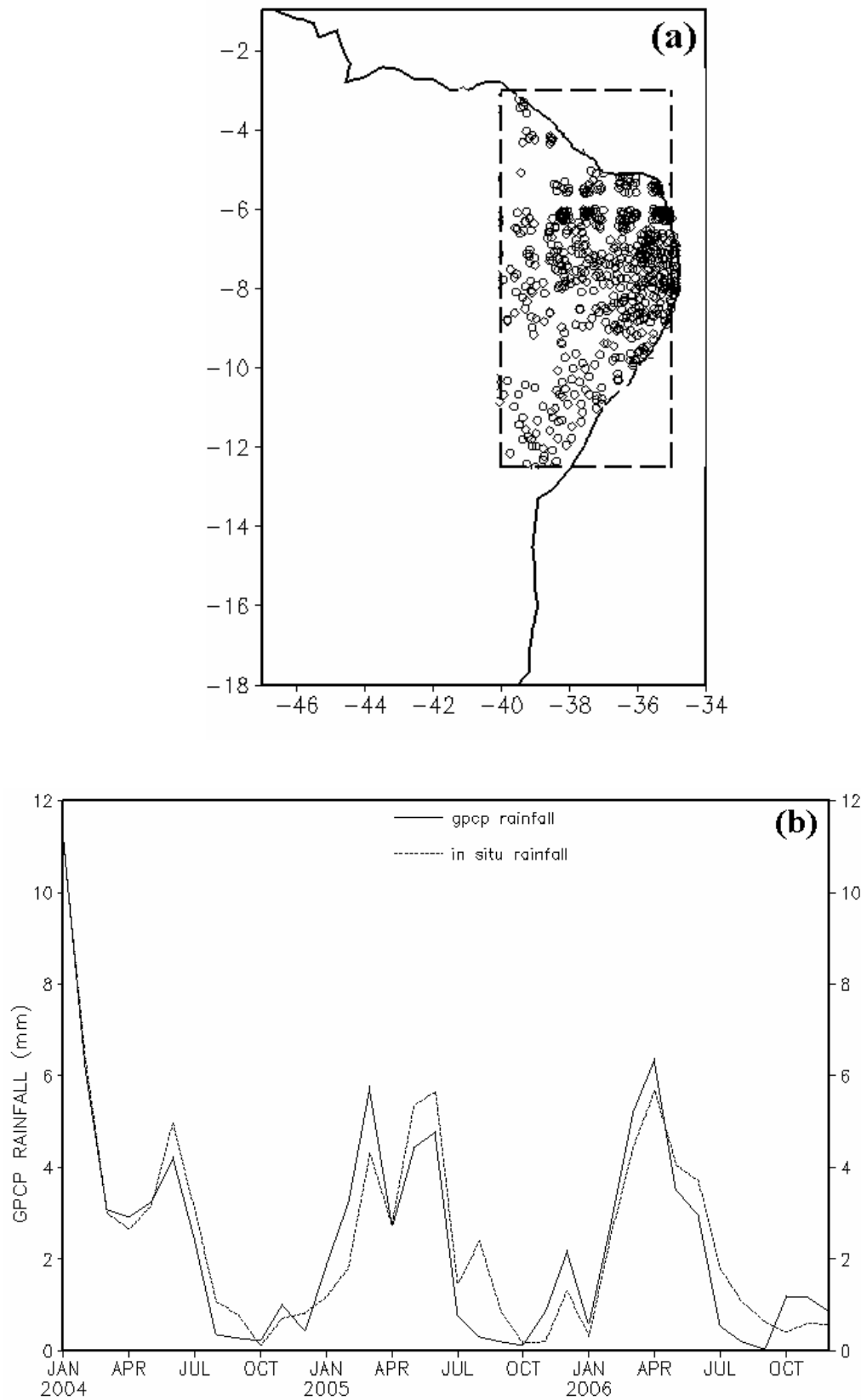


Figure 1: (a) Spatial distribution of 682 stations of the Nordeste. The dashed rectangle represents the eastern part of the Nordeste ranged between 40°W-35°W of longitude and 12.5°S-2.5°S of latitude. (b) GPCP and *in-situ* monthly rainfall 2004-2006 averaged over the Nordeste.

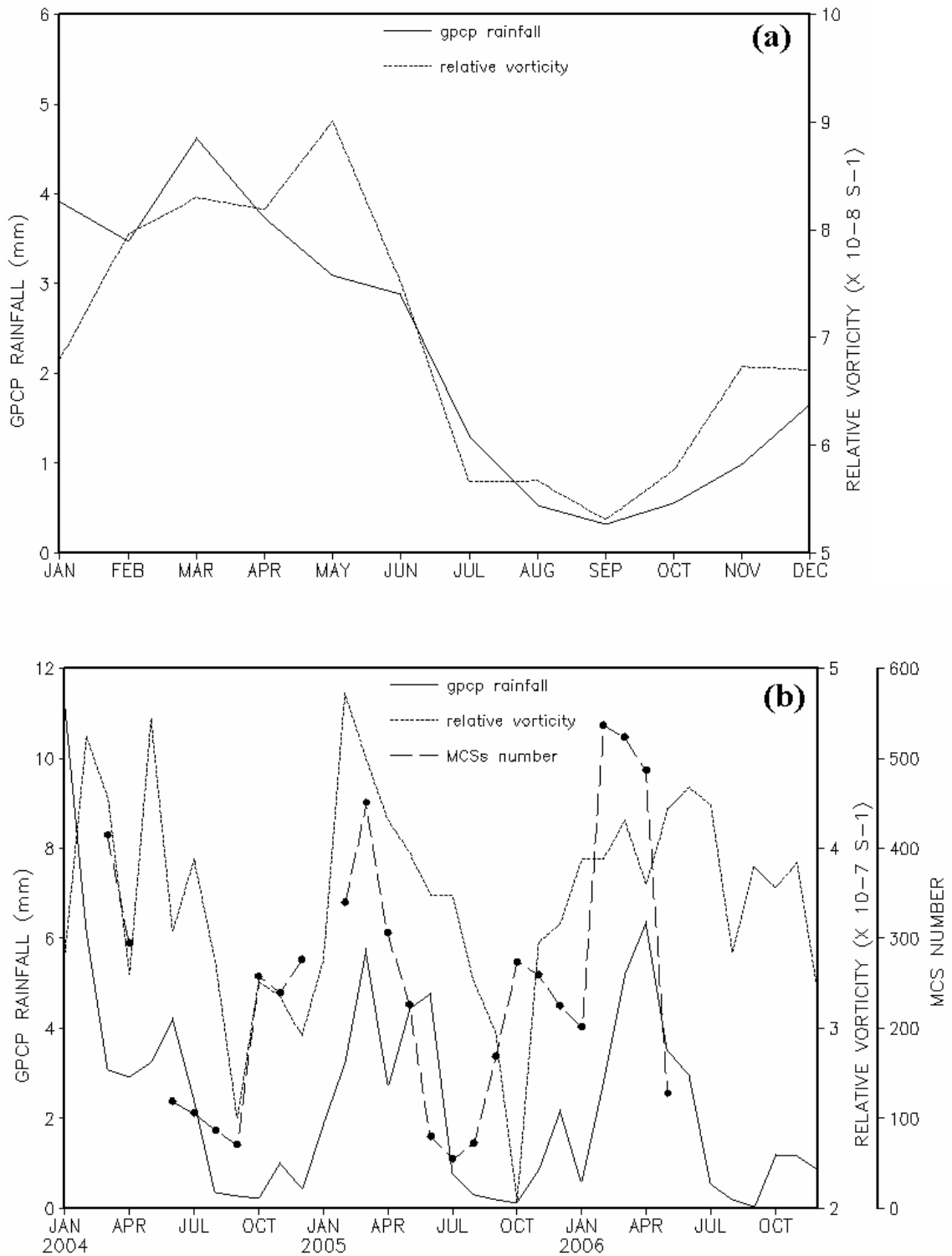


Figure 2: (a) Monthly climatology of GPCP rainfall (dotted line) during 1997-2006 calculated over the Nordeste and the 700 hPa positive vorticity (solid line) inside the area $40^{\circ}\text{W}-20^{\circ}\text{E}$, $12.5^{\circ}\text{S}-2.5^{\circ}\text{S}$ for the period 1948-2006. (b) Monthly number of MCSs (lifespan > 2 hours), which move westward (dashed) from 20°W up to the Nordeste and have a dissipation coordinate ranged between 12.5°S and 2.5°S during 2004-2006. Monthly rainfall of GPCP (solid line) on the Nordeste monthly vorticity (dotted) on the area $40^{\circ}\text{W}-20^{\circ}\text{E}$, $12.5^{\circ}\text{S}-2.5^{\circ}\text{S}$ are also plotted.

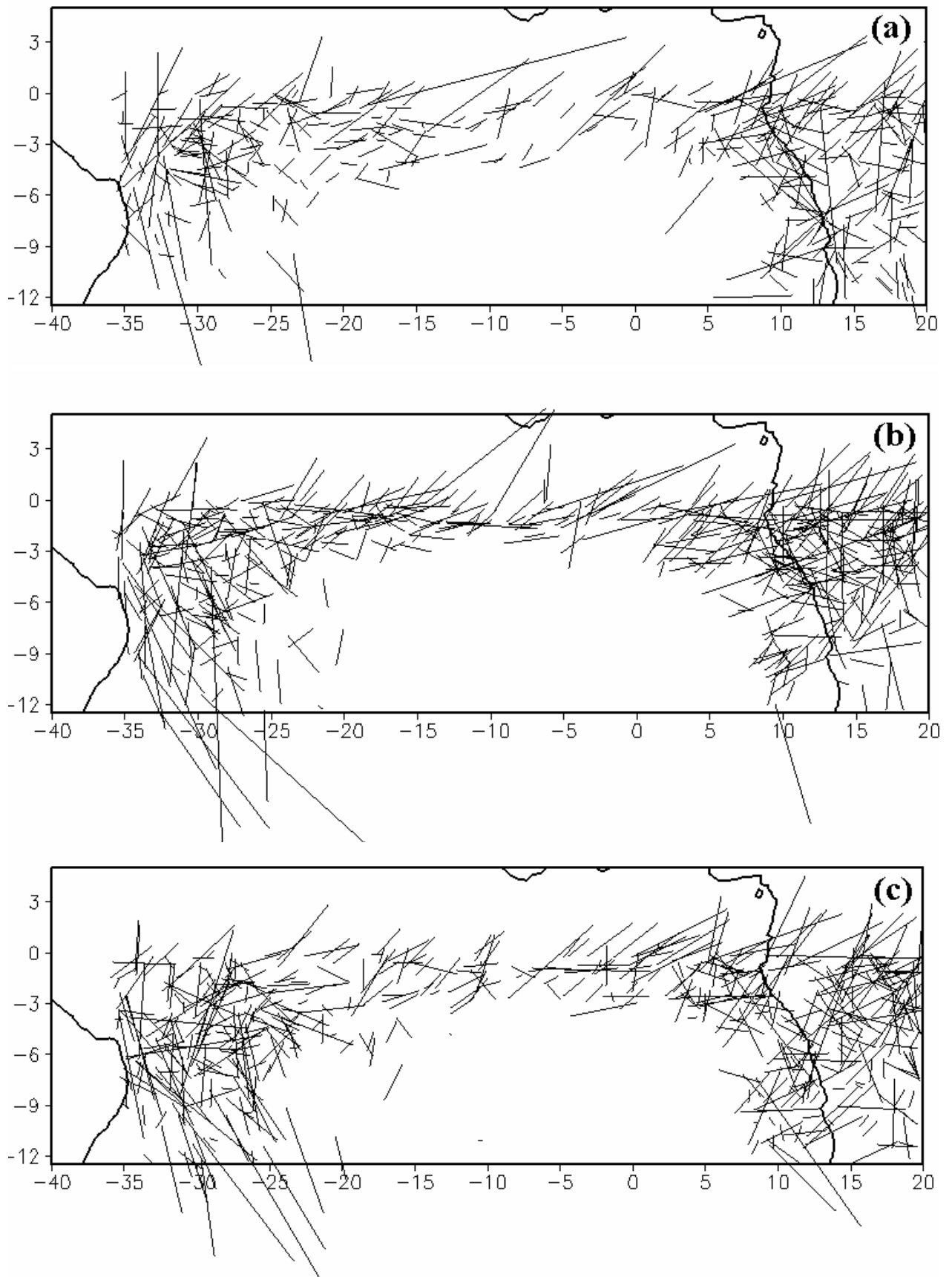


Figure 3: MCSS (> 10 hours) trajectories that move westward in the area 35°W-20°E, 12.5°S-5°N during January-May in (a) 2004, (b) 2005 and (c) 2006.

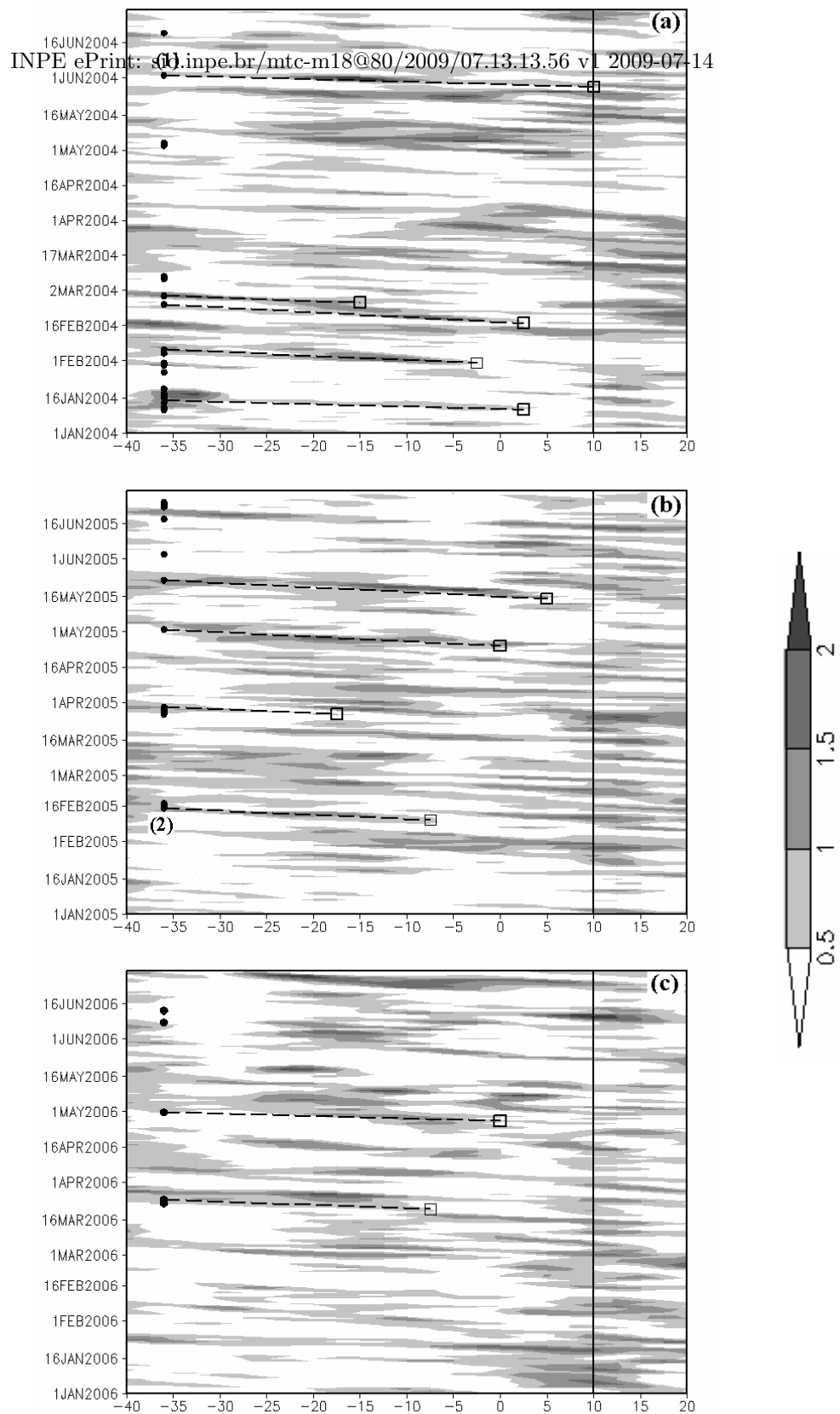


Figure 4 : The 700 hPa relative vorticity ($\times 10^{-3} \text{ S}^{-1}$) in January-June of (a) 2004, (b) 2005 and (c) 2006 along 40°W-20°E averaged between 12.5°S and 2.5°S. Rainfall positive anomalies up to 10 mm/day (black dots), calculated from the GPCP daily climatology, are represented at 36°W, *i.e.* on the mean eastern longitude of the *Nordeste*. Initiation coordinates of selected events are marked by squares. Event initiations and related strong rainy days are connected by a dashed line. The vertical line represents approximately the limit ($\sim 10^\circ\text{E}$) of the African continent.

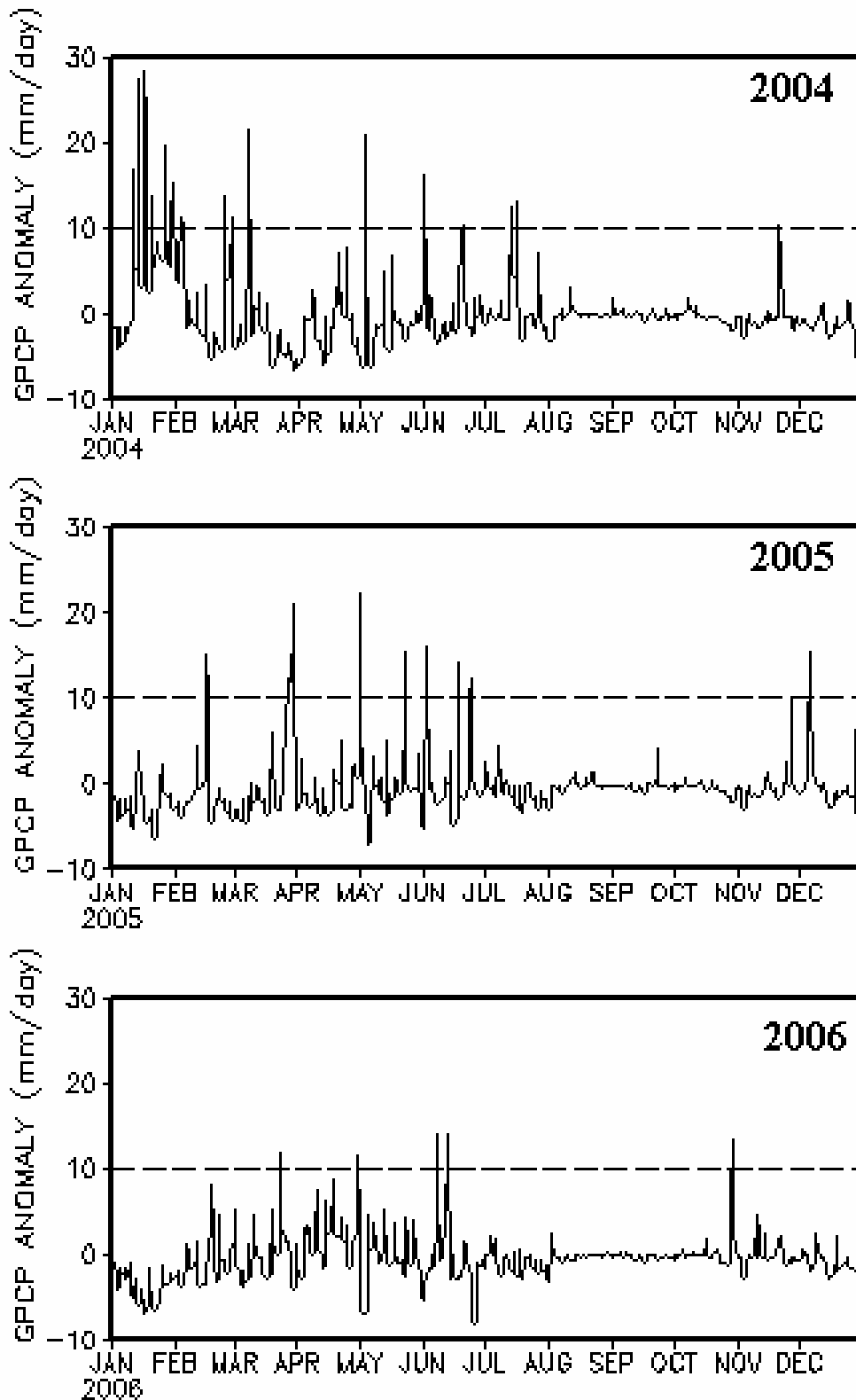


Figure 5: Chronological series of the daily GPCP anomalies calculated over the eastern Nordeste region (40°W - 35°W ; 12.5°S - 2.5°S) in 2004 (top), 2005 (middle) and 2006 (bottom). The horizontal dashed line represents the positive rainfall anomaly great to 10 mm/day. [ça serait bien ici d'indiquer par un symbole quelconque les 11 évènements sélectionnés]

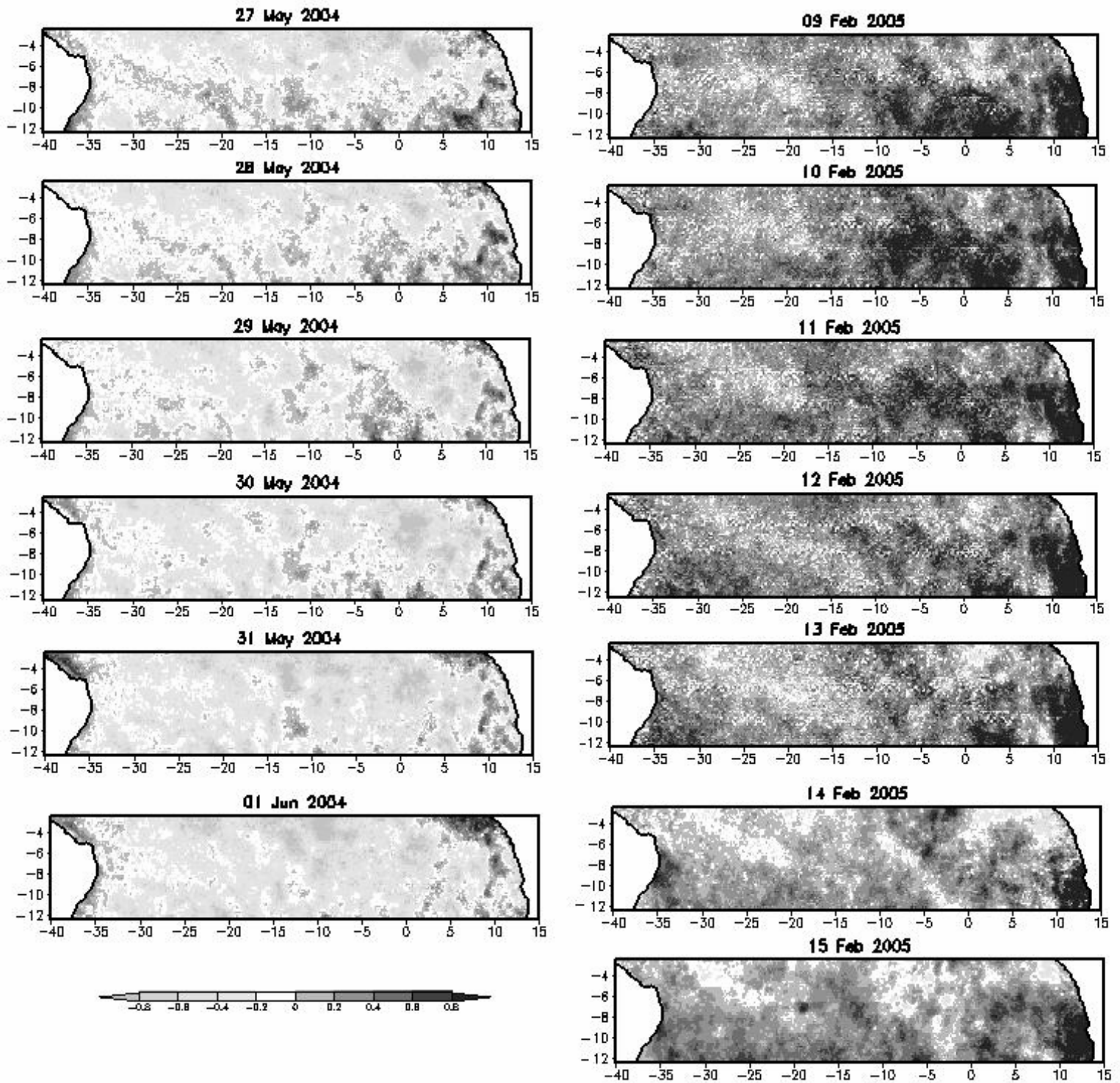


Figure 6: Daily evolution of the SST anomalies for the both events: (left) May 27-June 01 2004 and (right) Feb 09-Feb 15 2005 event. [\[mettre ces figures en couleur\]](#)

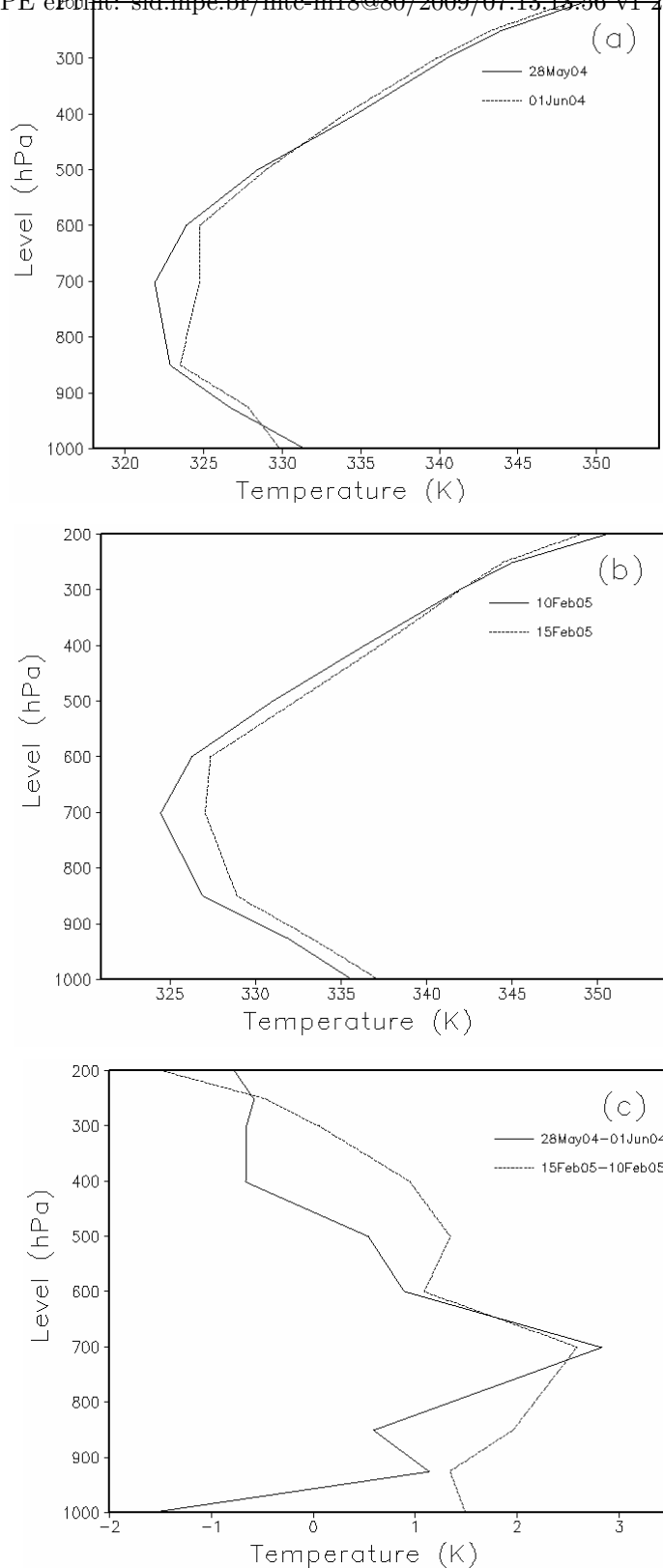


Figure 7: Vertical profiles of the equivalent potential temperature averaged over the oceanic domain 35°W-10°E; 12.5°S-2.5°S for two days during (a) the May 28 -Jun 01 2004 event and (b) the Feb 10-Feb 15 2005 event. Equivalent potential temperature curve for the initiation date of each event is continuous whereas it is dotted at the end. (c) Difference between the equivalent potential temperature at the end and at the initiation dates of each event: May 28 -Jun 01 2004 (solid) and Feb 10-Feb 15 2005 (dotted).

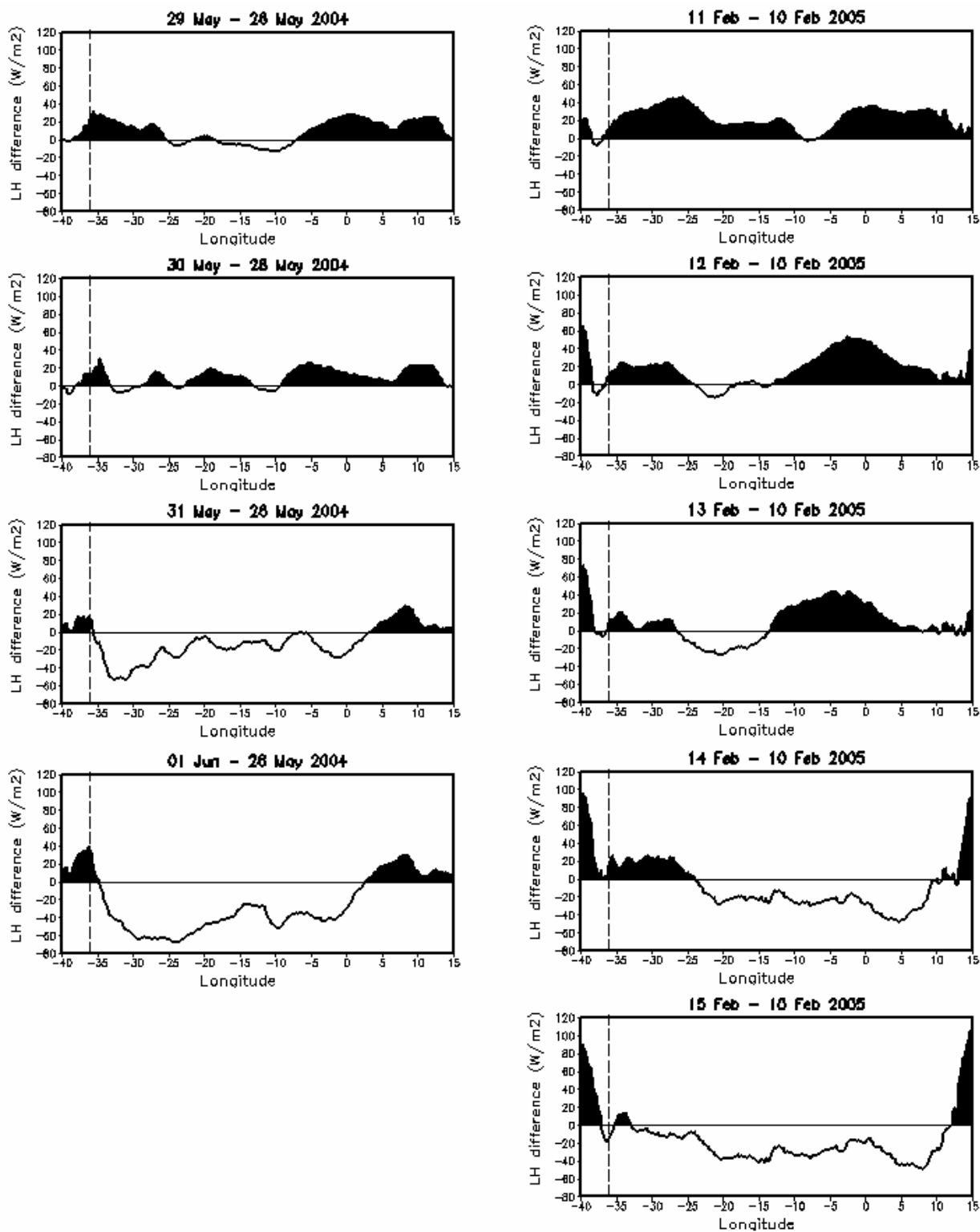


Figure 8: Daily evolution of the latent heat differences calculated over the 12.5°S-2.5°S latitudinal band along 40°W-15°E of longitude for the both events: (left) May 28 -Jun 01 2004 and (right) Feb 10-Feb 15 2005. Positive values are shaded. The vertical dashed line represents the mean longitude (~ 36°W) of the eastern Nordeste.

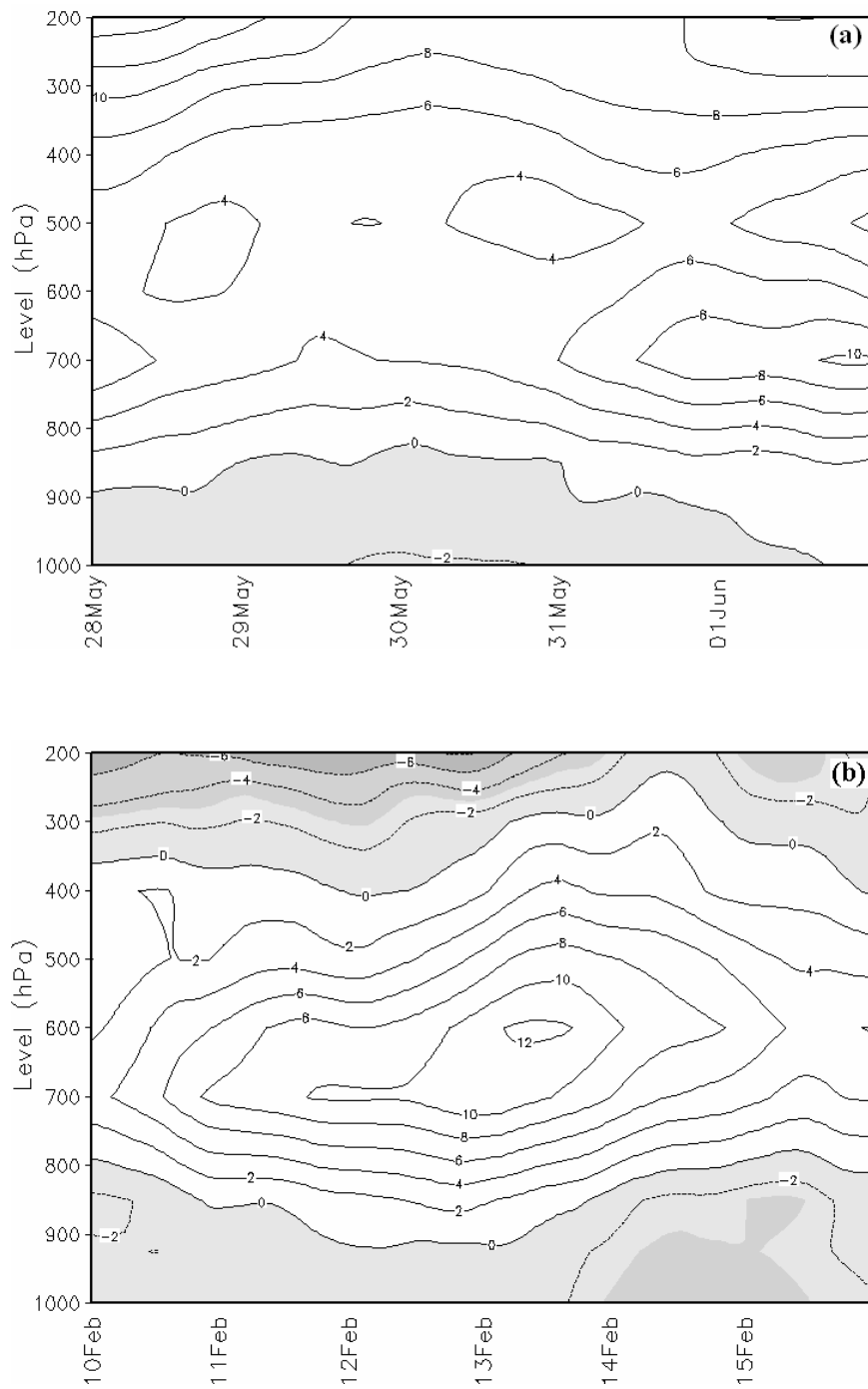


Figure 9: Hovmöller time-altitude diagram of the daily evolution of relative vertical vorticity ($\times 10^{-6} \text{ rad s}^{-1}$) calculated on the oceanic domain $35^{\circ}\text{W}-10^{\circ}\text{E}$; $12.5^{\circ}\text{S}-2.5^{\circ}\text{S}$ for the both events: (a) May 28-June 01 2004 and (b) Feb 10-Feb 15 2005. Negative values are shaded. [\[agrandir la fonte des valeurs numériques\]](#)

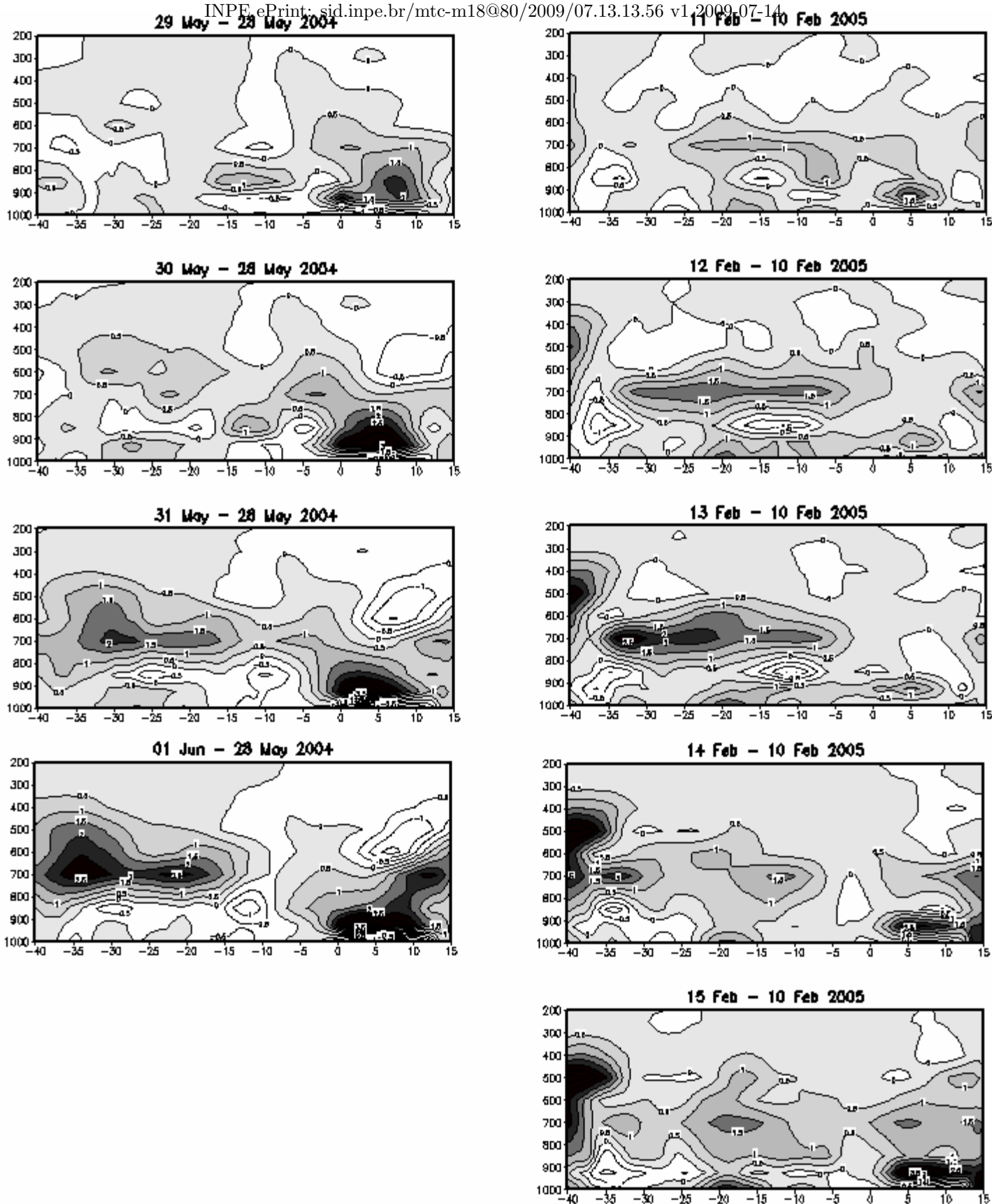


Figure 10: Hovmöller altitude-longitude diagram of the daily evolution of water vapour difference calculated on the 12.5°S-2.5°S latitudinal band along 40°W-15°E of longitude for the both events: (left) May 28-June 01 2004 and (right) Feb 10-Feb 15 2005. Positive values are shaded. [\[ameliorer et agrandir la fonte, mettre ligne 36W\]](#)

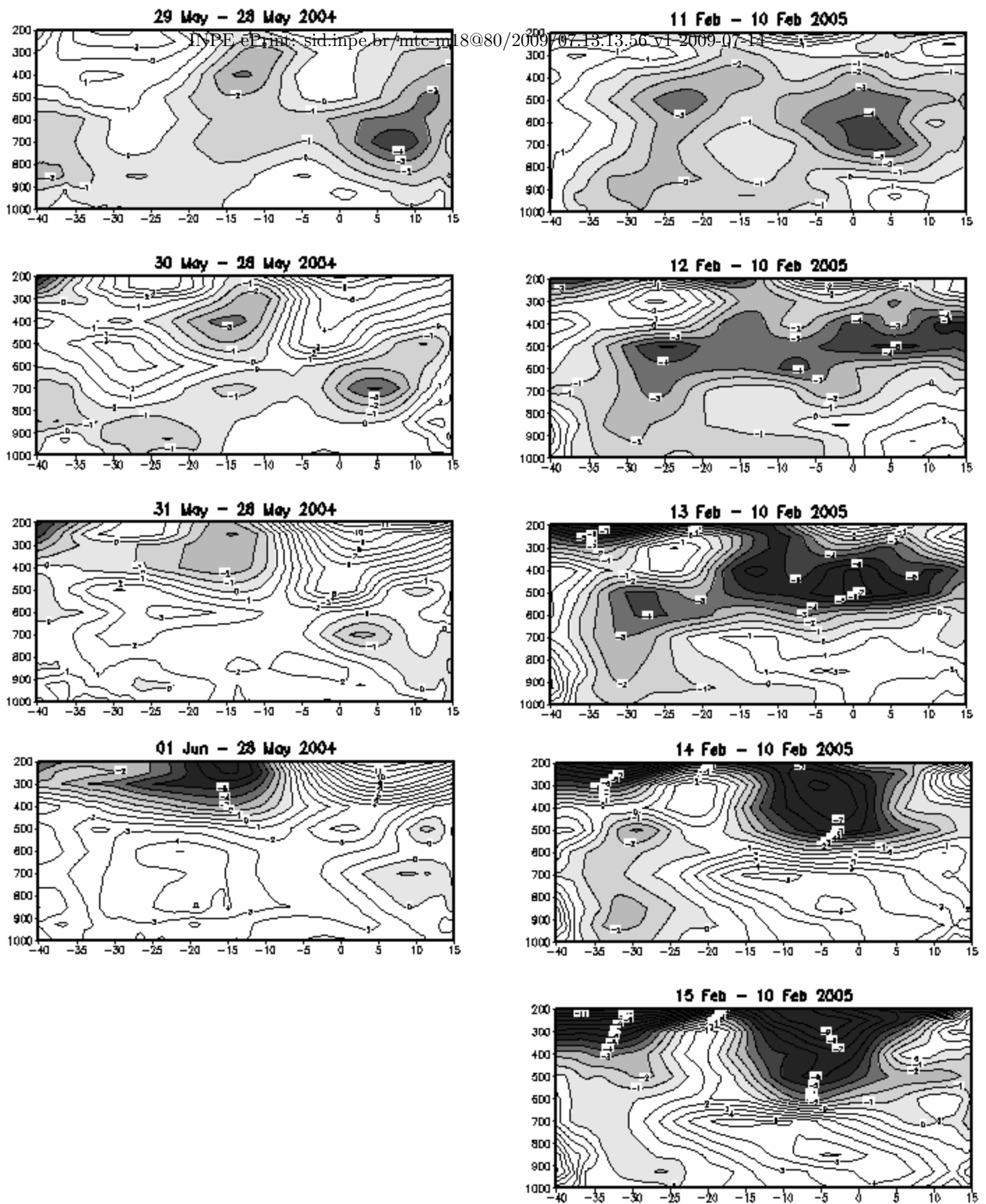


Figure 11: Hovmöller altitude-longitude diagram of the daily evolution of zonal wind differences calculated on the 12.5°S-2.5°S latitudinal band along 40°W-15°E of longitude for the both events: (left) May 28-June 01 2004 and (right) Feb 10-Feb 15 2005. Negative values are shaded. [[améliorer et agrandir la fonte, mettre ligne 36W](#)]

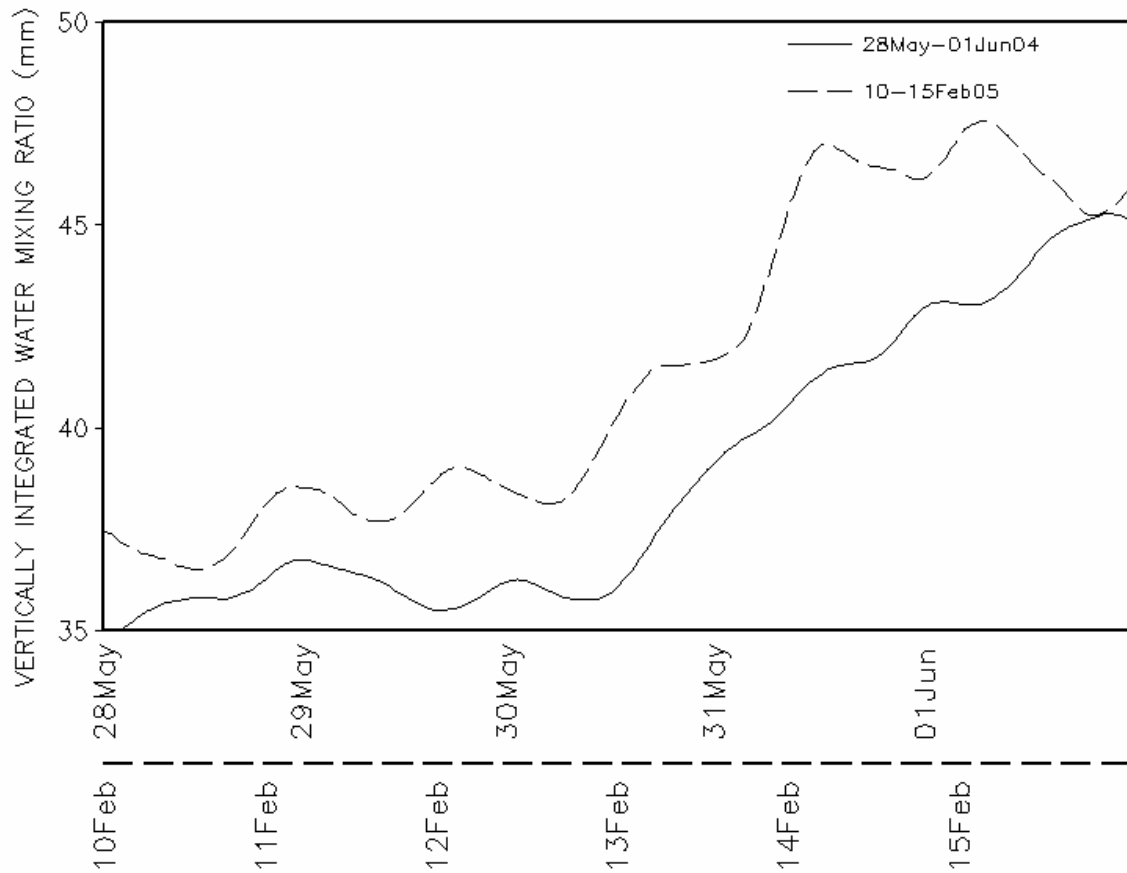


Figure 12: Daily evolution of the integrated water vapour mixing ratio (WVIR) calculated over the Nordeste (40°W - 35°W ; 12.5°S - 2.5°S) for the both events: May 28 - June 01 2004 (solid curve) and Feb 10-Feb 15 2005 (dashed curve). The daily scale for the period Feb 10-Feb 15 2005 (horizontal dashed line) is plotted at the bottom of the panel.

Table 1: Summary information for the 11 selected events in 2004, 2005 and 2006 when the strong anomaly of rain (> 10 mm) in the Nordeste is associated with AEWs. The mean virtual velocity (m s^{-1}), the initiation and rainy date of each event are also given.

Year	AEW Initiation Date	Date of Strong Rainfall	AEW Virtual Velocity (m/s)
2004	Jan 11	Jan 14	11.9
	Jan 31	Feb 04	8.3
	Feb 17	Feb 25	5.2
	Feb 25	Feb 28	8.5
	May 28	Jun 01	11.7
2005	Feb 10	Feb 15	7.0
	Mar 27	Mar 30	8.5
	Apr 25	May 02	5.7
	May 15	May 23	6.5
2006	Mar 20	Mar 23	8.8
	Apr 27	Apr 30	7.8
average			8.2